# Spectator response to the participant blast

L. Shi and P. Danielewicz
*National Superconducting Cyclotron Laboratory and Department of Physics and Astronomy, Michigan State University, East Lansing, Michigan 48824*

R. Lacey
*Department of Chemistry, State University of New York at Stony Brook, Stony Brook, New York 11794-3400*
(Received 4 May 2001; published 26 July 2001)

The interplay between spectator and participant matter in heavy-ion collisions is investigated in the context of a microscopic transport model. Transport simulations show that flow patterns for the participant matter are strongly influenced by the presence of the nearby spectator matter. However, the influence is mutual. During the explosion of the participant zone, the spectator matter acquires a transverse momentum $\langle P^x/A\rangle$ that shows sensitivity to the nuclear incompressibility and to the momentum dependence of the nuclear mean field (MF). An observed change in the net average momentum per nucleon, $\Delta|\langle \mathbf{P}/A\rangle|$, can be associated with the momentum dependence of the MF. For a momentum-dependent MF and a low impact parameter in a heavy system, the spectators may emerge faster than in the initial state, accelerated by the violent participant explosion. The average excitation energy and the mass of the spectators, in contrast to the momentum, show little sensitivity to the nuclear equation of state.

DOI: 10.1103/PhysRevC.64.034601 PACS number(s): 25.75.Ld, 25.70.−z, 21.65.+f

## I. INTRODUCTION

One of the major goals of intermediate and high-energy heavy-ion collision studies is the determination of the nuclear equation of state (EOS). The EOS constrains the nucleon-nucleon interactions in nuclear matter [1] and is an important ingredient for a detailed understanding of the supernovae explosions [2], the structure of neutron stars [3], and the evolution of the early Universe [4]. While the precise relationship between the EOS and the nucleon-nucleon interaction remains complicated [1], the EOS continues to be an important ingredient for developing an understanding for a range of nuclear processes including many heavy-ion reaction-phenomena [5].

Phenomenological parametrizations of the EOS are usually constrained with the properties of nuclear-matter at normal density $\rho_0$ and diverge at much higher densities that can be probed in energetic heavy-ion reactions. An important complication for heavy-ion collisions results from the fact that the duration of the initial high-density stage of the collision is very short compared to the time scale for the whole reaction process. For example, in an 800 MeV/nucleon $b=5$ fm collision of $^{124}\mathrm{Sn}+^{124}\mathrm{Sn}$, the high-density stage with a central density $\rho_c>1.5\rho_0$ lasts about 13 fm/$c$, while the elapsed time from the initial impact to the complete separation of target and projectile is $\sim 40$ fm/$c$. The spectator properties continue to develop well beyond this time [6]. Given the short duration of the high-density stage, signals which carry information about the high-density phase of the collision could be easily washed out by other signals generated at a later stage. In consequence, reaction simulations are needed to provide guidance for the measurement of signals which not only probe the high-density stage but survive through the entire duration of the collision process.

The collective flow of participants has been observed for a long time [7–9]. The flow is believed to result from early stage compression and an expansion [10–14], and can carry information on the initial high-density phase. The relation between the nuclear EOS and the flow phenomena has been explored extensively in simulations and a recent example is the analysis of the transverse-momentum dependence of the elliptical flow [15]. The elliptical flow is shaped by an interplay of geometry and mean field and, when gated by the transverse momentum, reveals the momentum dependence of mean field at supranormal densities.

The elliptical flow pattern of the participant matter is affected by the presence of the cold spectators [14–16], as will be reiterated. When nucleons are decelerated in the participant region, the longitudinal kinetic energy associated with the initial colliding nuclei is converted into the thermal and potential compression energy. In a subsequent rapid expansion or explosion, the collective transverse energy develops [12,13,10,11] and many particles from the participant region get emitted in the transverse directions. The particles emitted towards the reaction plane can encounter the cold spectator pieces and, hence, get redirected. In contrast, the particles emitted essentially perpendicular to the reaction plane are largely unimpeded by the spectators. Thus, for beam energies leading to a rapid expansion in the vicinity of the spectators, elliptic flow directed out of the reaction plane (squeeze-out) is expected. This squeeze-out is related to the pace at which the expansion develops, and is, therefore, related to the EOS.

On the other hand, since the spectators serve to deflect particle emissions toward the reaction plane, their properties may be significantly modified. This prompts us to analyze the characteristics of the spectators resulting from the collision process. In one sense, the spectators can be viewed as probes which were present at the site of the nuclear explosion leading to the rapid particle emission. Thus a careful study of their characteristics could complement the results from the elliptic flow and provide further information on the properties of high-density nuclear matter.

 

Long-time evolution of spectators has been studied in recent past by Gaitanos *et al.* [6]. A comprehensive summary of experimental results for spectators produced in reactions at different centralities has been presented by Pochodzalla [17]. In particular, universal features of spectator multifragmentation has been well documented [17,24]. The transverse momentum change of the spectator during a semicentral collision, to be addressed here, was looked at in the past via emulsions by Bogdanov *et al.* [18] (see also [19]). The systematics of the longitudinal momentum transfer to spectators in energetic reactions induced by light projectiles can be found in Ref. [20].

In this paper, we present an analysis of the interplay between participant and spectator matter during the violent stage of a heavy-ion reaction. We examine the impact of the interplay on the evolution of different physical characteristics within the two reaction zones. We investigate whether the spectator properties can be related in any fashion to the high-density EOS.

The paper is organized as follows. A brief description of our transport model is given in Sec. II. The reaction process and the participant-spectator interaction are described in Sec. III. The sensitivity of the emerging spectator characteristics to the nuclear EOS is investigated in Sec. IV. The paper is summarized in Sec. V.

## II. TRANSPORT MODEL

In this work, we utilize a set of transport equations of the Boltzmann-Uhlenbeck-Uehling (BUU) type to simulate semicentral heavy-ion reactions [5]. Within the approach, the reacting system is represented by quasiparticles with definite momentum and energy. Those quasiparticles move within the mean field (MF) produced by other quasiparticles and undergo collisions that represent fluctuations in the interaction with the medium beyond the mean field. With this, the phase-space distributions of quasiparticles, $f_X \equiv f_x(\mathbf{p},\mathbf{r},t)$, follow the set of equations:

$$\frac{\partial f_X}{\partial t}+\frac{\partial \epsilon_X}{\partial \mathbf{p}}\frac{\partial f_X}{\partial \mathbf{r}}-\frac{\partial \epsilon_X}{\partial \mathbf{r}}\frac{\partial f_X}{\partial \mathbf{p}}=\mathcal{K}_X^{<}(1\mp f_X)-\mathcal{K}_X^{>}f_X. \quad (1)$$

The left-hand side (LHS) in the above accounts for the changes in the distribution caused by the MF and the RHS for the changes in the distribution due to collisions. The single-particle energies $\epsilon_X$ are variational derivatives of the total system energy with respect to the phase-space distribution. The dependence of the total energy on phase-space distributions yields in the equilibrium the system EOS.

We carry out our calculations utilizing strongly momentum-dependent (MD) and momentum-independent (MI) MFs. In the calculations with the MI MFs, the energy density in the system is

$$e=\sum_X g_X\int\frac{d\mathbf{p}}{(2\pi)^3}f_X(\mathbf{p})\sqrt{p^2+m_X^2(\rho_s)}+\int_0^{\rho_s}d\rho_s' U(\rho_s') -\rho_s U(\rho_s), \quad (2)$$

TABLE I. Parameter values for the different mean fields utilized in the simulations. The first three columns refer to Eq. (4) and the next two to Eq. (6). The last column gives the Landau effective mass in normal matter at Fermi momentum.

| EOS | $a$ (MeV) | $b$ (MeV) | $\nu$ | $c$ | $\lambda$ | $m^*/m$ |
|---|---|---|---|---|---|---|
| S | 187.24 | 102.623 | 1.6340 | | | 0.98 |
| SM | 209.79 | 69.757 | 1.4623 | 0.64570 | 0.95460 | 0.70 |
| H | 121.258 | 52.102 | 2.4624 | | | 0.98 |
| HM | 122.785 | 20.427 | 2.7059 | 0.64570 | 0.95460 | 0.70 |

where $m_X(\rho_s)=m_X+A_X U(\rho_s)$, $A_X$ is baryon number and $\rho_s$ is scalar baryon density. The single-particle energy is then

$$\epsilon_X(p,\rho_s)=\sqrt{p^2+m_X^2(\rho_s)}, \quad (3)$$

and we parametrize the scalar field $U$ with

$$U(\rho_s)=\frac{-a(\rho_s/\rho_0)+b(\rho_s/\rho_0)^\nu}{1+\left(\frac{\rho_s}{2.5\rho_0}\right)^{\nu-1}}, \quad (4)$$

where $\rho_0$ is the normal density and $a$, $b$, and $\nu$ are parameters. In the calculations with MD MFs, the energy density is represented in the local baryon frame as

$$e=\sum_X g_X\int\frac{d\mathbf{p}}{(2\pi)^3}f_X(\mathbf{p})\left(m_X+\int_0^p dp' v_X^*(p',\rho)\right) +\int_0^\rho d\rho' U(\rho'). \quad (5)$$

The adopted form for $U(\rho)$ is the same as in Eq. (4) and the local particle velocity is parametrized with

$$v_X^*(p,\rho)=\frac{p}{\sqrt{p^2+\frac{m_X^2}{\left(1+c\frac{m_N}{m_X}\frac{A_X(\rho/\rho_0)}{(1+\lambda p^2/m_X^2)^2}\right)^2}}}. \quad (6)$$

With the above, the single-particle energy in the local frame is

$$\epsilon_X(p,\rho)=m_X+\int_0^p dp' v_X^*+A_X\left[\rho\left\langle\int_0^{p_1}dp'\frac{\partial v^*}{\partial\rho}\right\rangle+U(\rho)\right]. \quad (7)$$

The parameters for the MFs are given in Table I. Other details of our calculations, such as concerning the initialization of nuclei and the lattice Hamiltonian method for integrating the equations, can be found in Ref. [15]. For nucleon-nucleon collisions, a moderated elastic in-medium cross section is utilized through out this paper (same as Ref. [15]), unless otherwise indicated.

### III. SPECTATORS AND PARTICIPANTS

The important concept of spectators and participants in collisions was first introduced by Bowman *et al.* [21] and later employed for the description of a wide-angle energetic particle emission by Westfall *et al.* [22]. The two nuclei slamming against one other can be viewed as producing cylindrical cuts through each other. The swept-out nucleons or participants (from projectile and target) undergo a violent collision process. The remnants of the projectile and target, the spectators, continue in the meantime with largely undisturbed velocities, and are much less affected by the collision process than the participant nucleons. On one hand, this picture is supported by features of the data and, on the other, by dynamic simulations [23,12,13,6]. During the violent stage of a reaction the spectators can influence the behavior of participant matter. Specifically, the spectators can inhibit the collective transverse expansion of the decompressing participant matter and effectively shadow particle emission directed toward the reaction plane. A consequence of this shadowing is the observation of preferential squeeze-out of particles perpendicular to the reaction plane as illustrated below.

Figure 1 summarizes the results obtained from simulations of $^{197}$Au+$^{197}$Au collisions at a beam energy $T_{lab}=1$ GeV/nucleon and an impact parameter $b=8$ fm. Unless indicated otherwise, a hard momentum-dependent (HM) EOS (cf. Table I) was used. Figure 1(a) shows the time evolution of the density of both participant and spectator matter. The solid and dashed curves show, respectively, the baryon density $\rho_c$ at the center of the collision system (participants) and the baryon density in the local frame at the geometric center of the spectator matter $\rho_{spec}$. Here, the operational definition of spectator matter is that the magnitude of the local longitudinal velocity exceeds half of the velocity in the initial state and that the local density exceeds one-tenth of the normal density. The solid line in Fig. 1(a) clearly illustrates the rapid density build-up (for $t \leqslant 5$ fm/$c$) followed by expansion of the participant matter. The dashed line also points to a weak compression of the spectator matter during the expansion phase of the participants. The latter observation is consistent with the expected delay associated with the time it takes a compression wave to reach the center of the spectator matter, starting from an edge.

Figure 1(b) shows the time evolution of the elliptic flow parameter $v_2$ for all midrapidity particles. The parameter is defined as

$$v_2=\langle \cos(2\phi)\rangle, \tag{8}$$

where $\phi$ is the azimuthal angle in the $X$-$Y$ plane perpendicular to the beam axis $Z$; the $X$-$Z$ plane defines the reaction plane. The value of $v_2$ conveys information about the pattern of particle emission from the central participant region. The hot participant region has an initial elliptical shape in the $X$-$Y$ plane due to the overlap geometry. Since the long and short axes of the ellipse point in the $Y$ direction and in the $X$ direction, respectively, the matter starts out with stronger MF and pressure gradients in the $X$ direction. Given the shape of the emission source and the gradients, the matter is first expected to develop a stronger expansion in the $X$ direction

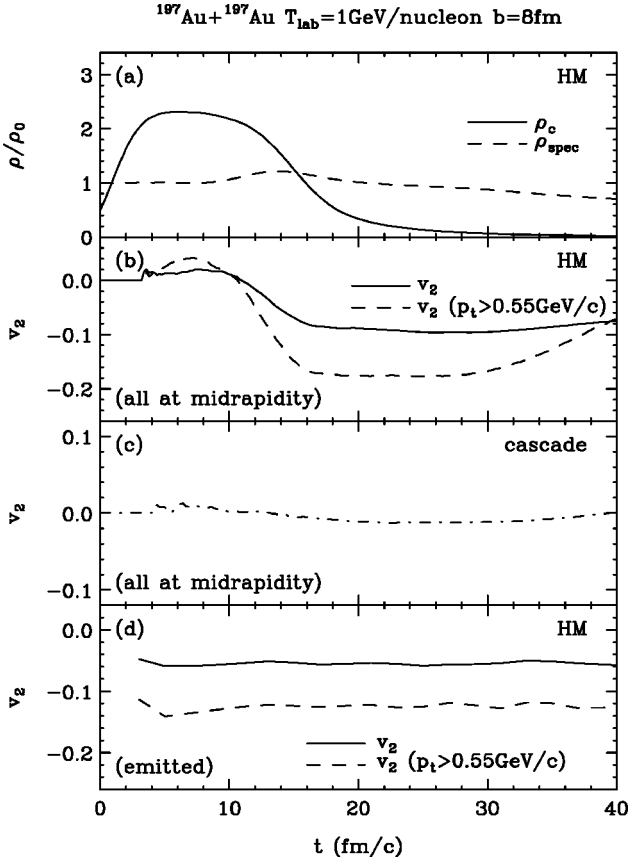


FIG. 1. Results from a BUU simulation of the $^{197}$Au+$^{197}$Au collision at 1 GeV/nucleon and $b=8$ fm, as a function of time: (a) the central densities of the participant $\rho_c$ and the spectator matter $\rho_{spec}$; (b)–(d) the midrapidity elliptical flow parameter $v_2$. The results are from a simulation with the HM mean field, except for those in the panel (c) which are from a simulation with no mean field. The panels (b) and (c) show the elliptic flow parameter for all particles in the system while (d) shows the elliptic flow for particles emitted in the vicinity of a given time. In the case of the HM calculations, also shown is $v_2$ when a high-momentum gate $p_t > 0.55$ GeV/$c$ is applied to the particles.

and, hence, to give rise to positive values of $v_2$. If the spectators are nearby during the expansion phase, they can serve to stall the expansion in the $X$ direction and a compression wave then develops within the spectator matter [cf. Fig. 1(a)]. The resulting dominant expansion of participant matter in the $Y$ direction gives rise to negative values of $v_2$. Figure 1(b) indicates that this preferential out-of-plane emission pattern begins after $\sim 7$ fm/$c$. The time correlation between the change in sign of $v_2$ and the decrease in the magnitude of the central density should be noted in the figure. The central density of participant matter $\rho_c$ begins to drop at about 7 fm/$c$ and the most rapid declines ends at $\sim 16$ fm/$c$; during this time the elliptical flow drops from its maximum positive value to its maximum negative value.

A comparison of Figs. 1(b) and 1(c) illustrates the important role of the MF in shaping the elliptical flow magnitude. Figure 1(c) shows the time dependence of $v_2$ obtained when the calculations are performed without the inclusion of a MF (cascade mode). In contrast to the evolution with the mean

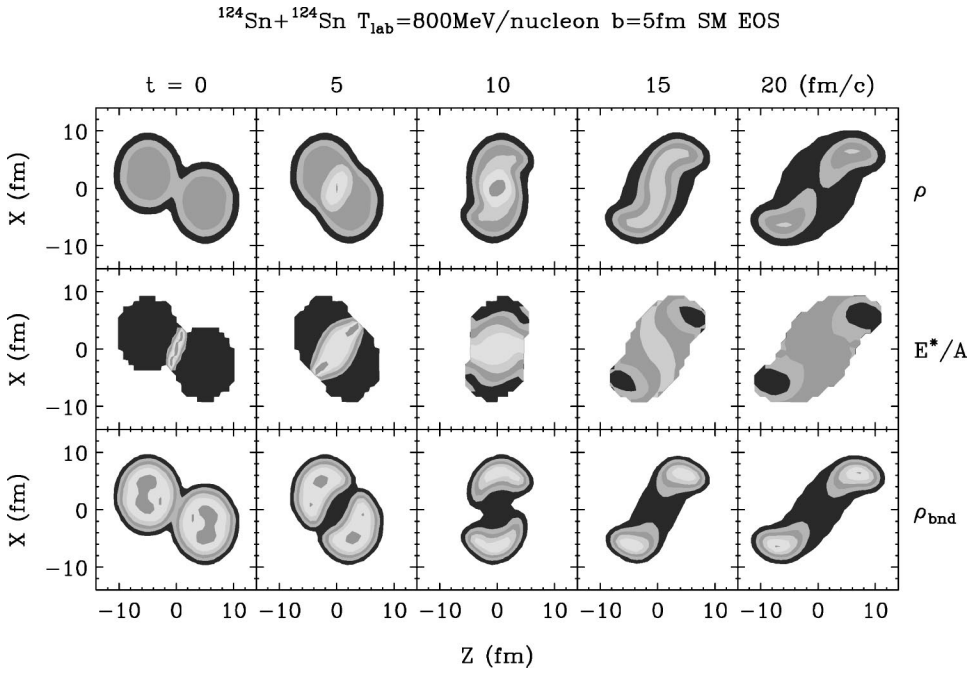


FIG. 2. Contour plots of the system-frame baryon density $\rho$ (top row), local excitation energy $E^*/A$ (middle row), and of the density of bound baryons $\rho_{\mathrm{bnd}}$ (bottom row), in the $^{124}\mathrm{Sn}+^{124}\mathrm{Sn}$ reaction at $T_{lab}=800$ MeV/nucleon and $b=5$ fm, at times $t=0$, 5, 10, 15, and 20 fm/$c$ (columns from left to right). The calculations have been carried out employing the soft momentum-dependent EOS. The contour lines for the densities correspond to the values, relative to the normal density, of $\rho$ from 0.1 to 2.1 with increment of 0.4. The contour lines for $\rho_{\mathrm{bnd}}$ are from 0.1 to 1.1 with increment of 0.2. The contour lines for the excitation energy correspond to the values of $E^*/A$ at 5, 20, 40, 80, 120, and 160 MeV. For statistical reasons, contour plots for the energy have been suppressed for the baryon densities $\rho<0.1\rho_0$. Note, regarding the excitation energy, that the interior of the participant region is hot while the interior of the spectator matter is cold.

field [cf. Fig. 1(b)] where $v_2$ first achieves significant positive and then negative values, Fig. 1(c) indicates $v_2$ values which stay close to zero over the entire time evolution of the system. This trend is related to the fact that in the cascade model the transverse expansion is slow compared to the time duration for which the spectators are in close proximity to the participant matter, or compared to the time required for longitudinal motion to thin the matter. The important role of the MF for the generation of elliptic flow and the sensitivity of this flow to the EOS has been stressed [14–16].

The temporal difference of $v_2$ for all midrapidity particles in the system, and for those particles that have left the system can be observed by comparing Figs. 1(b) and 1(d). Figure 1(b) shows the change in $v_2$ with time as discussed above. On the other hand, Fig. 1(d) indicates little or no change of $v_2$ (over time) for midrapidity particles that have left the system. That is, out-of-plane emission is favored (negative $v_2$) for all emission times. Figures 1(b) and 1(d) also show $v_2$ as a function of time for particles with transverse momentum $p_t>0.55$ GeV/$c$; these panels indicate that faster particles are more sensitive to the obstructions as well as to any directionality in the collective motion.

The analyses of elliptical flow and related works have established connections between features of the participant matter resulting from the participant-spectator interaction and the nuclear EOS [12,10,11,15,14,16]. On the other hand, it is not known whether the same interaction (during the violent stage of a reaction) leaves any lasting effects in the spectators that could be related to EOS. Extensive studies of the statistical behavior of spectator matter have been carried out [17,24] for time scales which are long compared to the collision time. Such studies do not address the dynamical impact of the violent reaction stage on spectators. During the violent stage of a collision, the spectators remain close to the participant matter, so they might serve as a good sensor for the explosion. Thus, we proceed to take a closer look at the changes which may occur in the spectator matter following their interaction with the participants. In addition we investigate whether or not such changes have a connection to the EOS.

Figure 2 shows contour plots of different quantities within the reaction plane now from $^{124}\mathrm{Sn}+^{124}\mathrm{Sn}$ reaction simulations at the beam energy of $T_{\mathrm{lab}}=800$ MeV/nucleon, at the impact parameter $b=5$ fm, carried out with a soft momentum-dependent (SM) mean field. The columns from left to right represent the reaction at 5 fm/$c$ time increments. The top and middle rows show the baryon density in the system frame $\rho$ and the local excitation energy $E^*/A$, respectively. The bottom row shows the density $\rho_{\mathrm{bnd}}$ of baryons that are bound in their local frame ($\epsilon_X<m_X$). As may be expected, the excitation energies reach rather high values in the participant region but remain low within the spectator region throughout the violent stage of the reaction. Most of the particles in the participant region are found to be unbound, i.e., $\rho_{\mathrm{bnd}}$ is low. On the other hand, most of the particles within the spectator region are bound. They move with velocities that are close to each other, and this keeps $\rho_{\mathrm{bnd}}$ sizable throughout the violent collision stage.

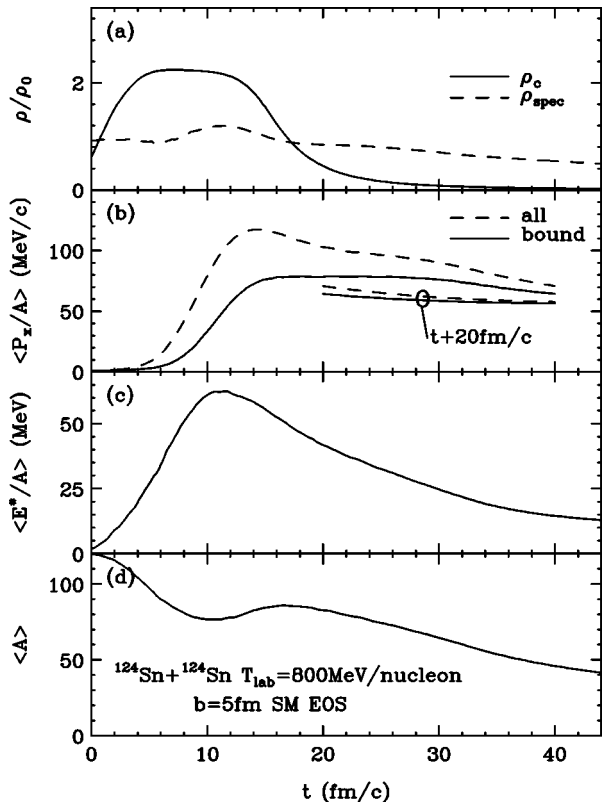


FIG. 3. Evolution of selected quantities in the $^{124}$Sn+$^{124}$Sn reaction at 800 MeV/nucleon and $b=5$ fm, from a calculation with a soft momentum-dependent EOS. The panel (a) shows the density at the center of a spectator $\rho_{\rm spec}$ (dashed line) together with the density at the system center $\rho_c$ (solid line). The panel (b) shows the average in-plane transverse momentum per nucleon of the spectator $\langle P^X/A\rangle$ calculated using all spectator particles (solid line) and using only bound spectator particles (dashed line). Two extra lines in the panel show evolution of the momenta past the 40 fm/$c$ of the abscissa. The panels (c) and (d) show, respectively, the spectator excitation energy per nucleon $\langle E^*/A\rangle$ and the mass number $\langle A\rangle$ from all spectator particles.

Figure 3 provides next a detailed time development of the selected quantities in the 800 MeV/nucleon $^{124}$Sn+$^{124}$Sn system for which the contour plots were given. Figure 3(a) displays the evolution of baryon density at the system center, $\rho_c$, and of baryon density at the center of the spectator region, $\rho_{\rm spec}$. The high-density stage for the participant matter in Fig. 3(a), characterized by $\rho_c > \rho_0$, lasts over a time that is short in comparison to the time needed for a clear separation of the target and projectile spectators from the participant zone, cf. Fig. 2. To observe a stabilization of the spectator properties we needed to follow the particular reaction up to $\sim$60 fm/$c$. Longer-term studies of the spectator development have been carried out within the BUU approach [6]. However, as the spectators approach equilibrium, they might be described in terms of the statistical decay method owning at this stage advantages over the BUU equation.

Figure 3(b) shows the average transverse momentum per nucleon of the spectator, in the reaction plane, as a function of time. In calculating the average, we can include all spectator particles as specified before (dashed line in the panel) or the subset of particles that are bound in the local frames (solid line). The averages, obviously, approach the same asymptotic value over time, but the approach is faster for the bound-particle average. Note that the extra lines in Fig. 3(b) represent the evolution of the average momenta past the 40 fm/$c$ of the abscissa. Calculated in either manner, the spectator average momentum $\langle P^X/A\rangle$ reaches its magnitude during the high-density stage in the participant matter and only somewhat reduces to stable during the expansion that follows. This suggests that the spectators can, indeed, provide information on the high-density stage of the collision.

Figure 3(c) shows the average excitation energy per nucleon $\langle E^*/A\rangle$ of the spectator as a function a time. Within the studied time interval, the excitation energy rapidly rises and decreases and then changes at a slower pace. During the violent reaction stage, some particles traversing from the participant into the spectator matter contribute to the excitation of the spectator matter. As time progresses, some of those particles will travel through the matter and leave the spectators. Some other will degrade their energy within the spectator frame. (Note: we consistently continue with definition where the spectator matter is that for which the c.m. local velocity is larger than half the beam velocity and the local density exceeds the tenth of normal.)

Figure 3(d) shows the mass number of a spectator region as a function of time. The spectator mass number decreases rapidly as particles dive into the participant region and then the mass recovers somewhat, around the time of 20 fm/$c$, as some particles get through the opposite moving corona matter and join the bulk of the spectator matter moving along the beam direction. Later, a gradual deexcitation slowly reduces the spectator mass.

We have demonstrated in this section the interplay between the participants and spectators. We have shown how the elliptic flow is generated due to that interplay and how the interplay affects the spectator characteristics. In the next section we explore the sensitivity of spectator characteristics to the EOS for the nuclear matter in collision.

## IV. SPECTATOR SENSITIVITY TO THE NUCLEAR EQUATION OF STATE

In the light that the changes of the spectator properties could probe the compression and explosion of the participant matter, we follow the reaction simulations till a clear separation of the spectators from the participant matter and a stabilization of the spectator characteristics. We explore the sensitivity of the emerging spectator properties to different assumptions on the nuclear EOS. The results could serve to initialize statistical decay calculations for a complete description of a reaction.

In the following, we shall present a sample of our spectator investigations, within the $^{124}$Sn+$^{124}$Sn system in the beam energy range of 250 MeV/nucleon to 1 GeV/nucleon at impact parameters $b=5-7$ fm. We shall also quote results from $^{197}$Au+$^{197}$Au at 1 GeV/nucleon. We utilized four different EOS explored in the past, of which the parameters are given in Table I. We concentrated on the quantities that could be experimentally determined for the spectator, and thus the

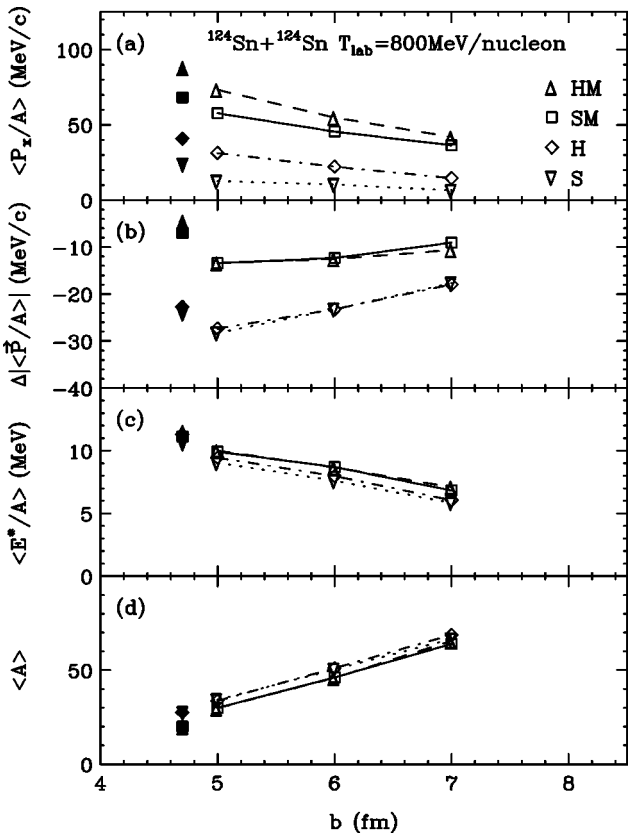


FIG. 4. Spectator properties in the 800 MeV/nucleon $^{124}$Sn $+^{124}$Sn collisions, as a function of the impact parameter, for four representative EOS: hard momentum-dependent (HM), soft momentum-dependent (SM), hard momentum-independent (H), and soft momentum-independent (S). The panel (a) shows the average in-plane transverse momentum of the spectator per nucleon $\langle P^X/A\rangle$. The panel (b) shows the change in the average net c.m. momentum per nucleon $\Delta|\langle \mathbf{P}/A\rangle|$. The panel (c) shows the average excitation energy per nucleon $\langle E^*/A\rangle$, and, finally, (d) shows the average spectator mass $\langle A\rangle$. Open symbols represent results obtained with reduced in-medium nucleon-nucleon cross sections; filled symbols represent results obtained at $b=5$ fm with free cross sections.

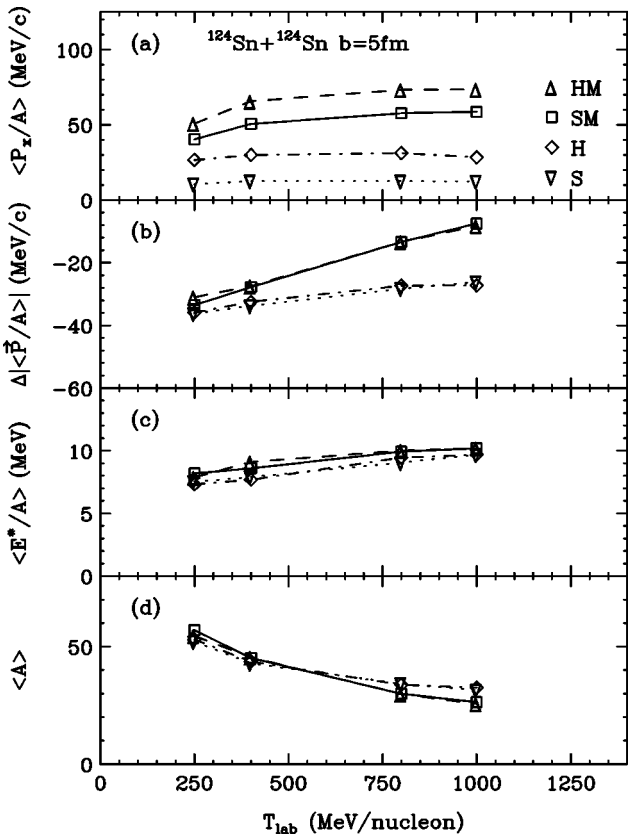


FIG. 5. Spectator properties in the $^{124}$Sn+$^{124}$Sn collisions at $b=5$ fm, as a function of the beam energy, for four representative EOS: hard momentum-dependent (HM), soft momentum-dependent (SM), hard momentum-independent (H), and soft momentum-independent (S). Panel (a) shows the average in-plane transverse momentum of the spectator per nucleon $\langle P^X/A\rangle$. Panel (b) shows the change in the average net c.m. momentum per nucleon $\Delta|\langle \mathbf{P}/A\rangle|$. Panel (c) shows the average excitation energy per nucleon $\langle E^*/A\rangle$. Finally, panel (d) shows the average spectator mass $\langle A\rangle$.

average transverse momentum per nucleon $\langle P^X/A\rangle$, the change in the average c.m. momentum per nucleon $\Delta|\langle \mathbf{P}/A\rangle|$, the average excitation energy per nucleon $\langle E^*/A\rangle$, and the average mass $\langle A\rangle$ following the violent stage of the reaction. The change in the average c.m. momentum is $\Delta|\langle \mathbf{P}/A\rangle| = \sqrt{\langle P^X/A\rangle^2+\langle P^Z/A\rangle^2}-(P/A)_i$.

The above mentioned quantities, towards the end of our simulations, are shown as a function of the impact parameter at $T_{\rm lab}=800$ MeV/nucleon in Fig. 4, by open symbols, and as a function of the beam energy at $b=5$ fm in Fig. 5, respectively. The resulting spectator $\langle P^X/A\rangle$ exhibits a clear sensitivity to the stiffness of EOS. We can see in both figures that a stiffer EOS results in a stronger sidewards push to the spectator. However, even more prominent is the sensitivity to the momentum dependence of the mean field. A strong momentum dependence results in a stronger push to the spectator than the lack of such dependence. Recall that the interplay between the spectator and the participant matter generates also the elliptic flow for the participant matter and it was possible to exploit the latter in the determination of the mean-field momentum dependence at supranormal densities [15,16].

The final momentum of the spectator reflects the momentum exchanges with the participant zone throughout the reaction. Initially, the nucleons from the opposing nucleus move nearly exclusively along the beam axis relative to the spectators. As equilibration progresses, the momenta in the participant zone acquire a level of randomness. Random exchanges of momentum between spectators and participants generally would drive the spectator momentum towards the average for the system, i.e., zero. However, the participant nucleons reach the spectators moving away from the system center, coming with momentum directed on the average outward, delivering an outward push to the spectator pieces.

The order of magnitude for the transverse push may be obtained from a simple estimate. Thus, in Sn+Sn at 800 MeV/nucleon, taking for the pressure in the compressed region from the nonrelativistic ideal-gas estimate,

$$p \simeq \rho \frac{2}{3} T_{\rm lab}/4A, \tag{9}$$

with $\rho \sim 2\rho_0 \sim 2/6$ fm$^{-3}$, we get $p \sim 40$ MeV/fm$^3$. The size of the high-density region in the $X$-$Z$ plane for Sn+Sn at medium $b$ is $\sim 4$ fm, cf. Fig. 2. The push to the spectator is then of the order of

$$P^x \approx pS\Delta t, \tag{10}$$

where $S$ is the transverse area pushed by the participant matter and $\Delta t$ is the duration of the push. With $S = \pi R^2/4 \sim 13$ fm$^2$ and $\Delta t \sim 5$ fm/$c$, cf. Figs. 2 and 3, we get

$$\frac{P^x}{A} = \frac{40\ \text{MeV/fm}^3 13\ \text{fm}^2\ 5\ \text{fm}/c}{50} \simeq 50\ \frac{\text{MeV}}{c}. \tag{11}$$

This appears to agree as to the general magnitude with what is found in the simulations. When the impact parameter increases, the fireball pressure decreases while the spectator mass increases. Thus, the momentum per nucleon decreases. With regard to the beam energy variation in the simulations, at low energies the pressure in the fireball region drops, resulting in smaller push to the spectators, with some compensation coming from a longer time for the spectators in the reaction zone and a longer fireball lifetime. With the rise in the beam energy from the low energy end, the rise in the transverse fireball pressure is moderated by the pion production and an increasing transparency. The spectator time in the vicinity of the explosion continuously drops resulting in a level of saturation in the spectator momentum per nucleon.

With regard to the changes in the magnitude of the c.m. momentum per nucleon $\Delta|\langle \mathbf{P}/A \rangle|$, we see in Figs. 4 and 5 that the results for MD MFs significantly differ from the results for MI MFs for Sn+Sn, with the latter MFs giving more momentum loss. The spectator mass and excitation energy, in contrast to the momentum, are rather insensitive to the MF in the present system.

While the results discussed till now have been obtained with reduced in-medium nucleon-nucleon cross sections [15], we also carried out calculations with the free nucleon-nucleon cross sections. The latter calculations for the same system at $T_{\rm lab} = 800$ MeV/nucleon $b = 5$ fm, are represented by filled symbols in Fig. 4. With free cross sections, the remnant masses are a bit lower, the excitation energies are higher, and so is the transverse push. The transverse push is more sensitive to the change in the EOS, than to the change in cross section, as evident in the figure. Contrary to what one might naively expect, less momentum per nucleon is lost in the free cross section case. We will come back to the last issue later.

In investigating the differences in results for the different EOS, we obviously looked at the details in the time development of the systems for the different EOS. Figure 6 shows the central participant density as a function of time. For the hard momentum-independent EOS a maximal density is reached earlier and the expansion sets faster than for the soft momentum-independent EOS. The S EOS allows for a higher compression than the H EOS. An MD EOS allows for a lower compression than a corresponding MI EOS. Moreover, the expansion develops earlier for an MD EOS than a corresponding MI EOS. Evidently, the momentum dependence plays a similar role to the stiffness of nuclear matter; it renders the matter less compressible in a dynamic situation.

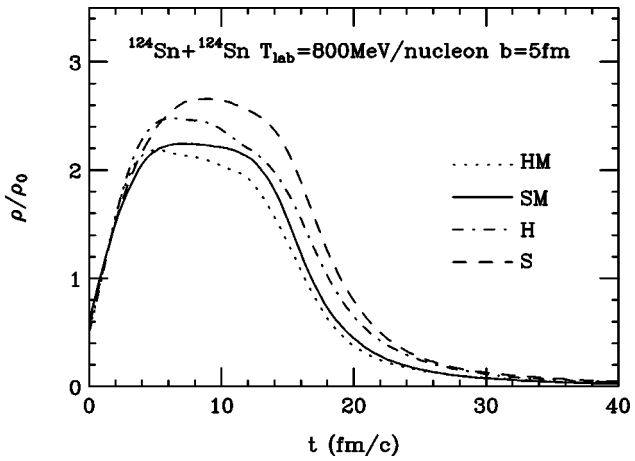


FIG. 6. Baryon density as a function of time at the center of the $^{124}$Sn+$^{124}$Sn system at $T_{\rm lab} = 800$ MeV/nucleon and $b = 5$ fm, for different MF's.

Figure 7 shows next the spectator transverse momentum in the $X$ direction as a function of time. As we have already pointed out before, the spectator transverse momentum per nucleon rises within a relatively short time interval. The rise starts about at the time when the maximal density is reached at the participant center; the rise stops due to combined effects of the spectator passing by and of the dilution of the participant zone. While there are up to 2 fm/$c$ differences in the start and end of the rise interval in Fig. 7, it is apparent that the differences in the final $\langle P^X/A \rangle$ must be due to the differences in magnitude of the transverse pressure (transverse momentum flow) for the different EOS and not in the duration of the rise. In fact, the slopes of the dependence of transverse momentum on time differ considerably more than do the final transverse momenta. A faster dilution for the more incompressible EOS shuts off the momentum rise sooner than for the more compressible EOS and moderates the differences in the final spectator momenta. Figure 8

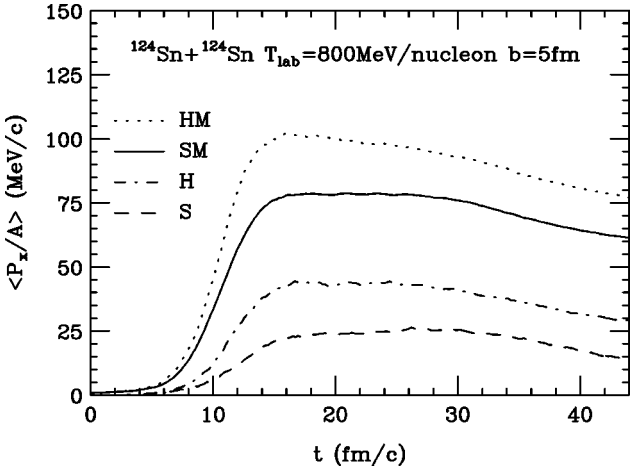


FIG. 7. Average in-plane transverse momentum per nucleon of a spectator in $b = 5$ fm $^{124}$Sn+$^{124}$Sn collisions at $T_{\rm lab} = 800$ MeV/nucleon, as a function of time, for different EOS.

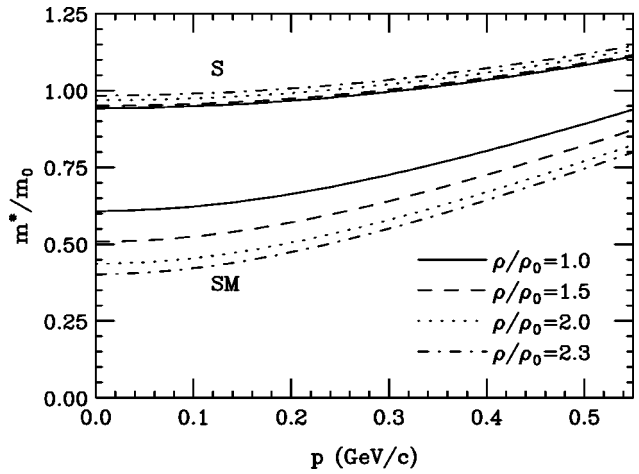


FIG. 8. Landau effective mass $m^*=p/v$, in units of free nucleon mass, as a function of momentum at several densities in cold nuclear matter for S and SM MF's.

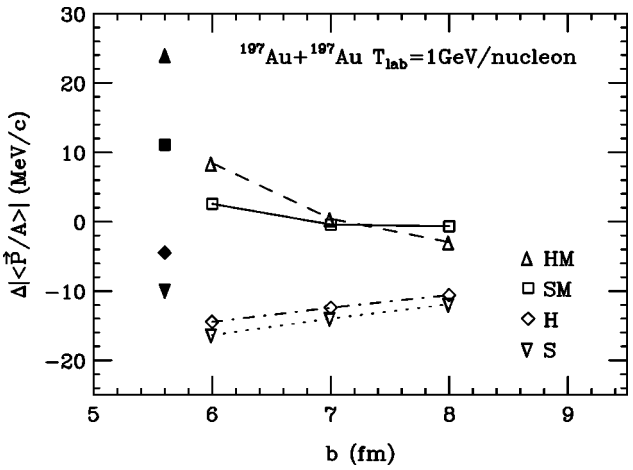


FIG. 9. The change in the net average c.m. momentum per nucleon $\Delta|\langle \mathbf{P}/A \rangle|$ of the spectator in the $^{197}$Au+$^{197}$Au system at $T_{lab}=1$ GeV/nucleon. Open symbols represent results obtained with reduced in-medium nucleon-nucleon cross sections; filled symbols represent results obtained at $b=6$ fm with free cross sections. A negative value of $\Delta|\langle \mathbf{P}/A \rangle|$ indicates a spectator deceleration, while a positive value indicates a net acceleration.

shows differences in the Landau effective mass, $m^*=p/v$, in cold nuclear matter at different densities for MI and MD MFs. Lower masses for the MD MF means that particles move out faster at same momenta.

The change in the magnitude of the c.m. momentum per nucleon $\Delta|\langle \mathbf{P}/A \rangle|$ is generally dominated by the change in the longitudinal momentum per nucleon. In Figs. 4 and 5 the net momentum per nucleon is seen to decrease in the Sn+Sn reactions under all conditions. That change in the momentum might be considered a measure of the friction involved in the interaction of the spectator with the participant zone. The friction is due to mentioned random changes of momenta in collisions between participants and spectators that, besides knocking particles off spectators, over time drive the average momentum towards the system average of zero. When examining the net spectator momentum per nucleon as a function of time in the Sn+Sn reactions, the momentum is first found to decrease but then found to recover somewhat. The late increase and part of the early momentum decrease could partly be attributed to our inability of cleanly separating the spectators from the participants, other than by a convention; the particles are intermittently intermixed and then separate.

The above view on the net spectator momentum, however, needs to be revised once the changes in the momentum are examined in the Au+Au system. The change in the net momentum per nucleon is shown for 1 GeV/nucleon reaction as a function of the impact parameter in Fig. 9, by open symbols for the in-medium reduced cross section. For low impact parameters and MD MFs, the average spectator momentum per nucleon increases in the reaction simulations.

The speeding up of the spectator at low $b$ in Au+Au may be, again, understood in terms of the explosion of the participant zone. On one hand, the spectator acquires the transverse momentum. On the other, in the longitudinal direction the explosion acts more on the rear of the spectator piece than on the front. If the explosion is strong enough, the ordered push may overcome the friction effects, producing a net longitudinal acceleration for a piece. There is no issue of energy conservation since the work is done by the participant on the spectator zone. The difference between Sn+Sn and Au+Au is in the equilibration time scale relative to the duration of the fireball. Differences in the net final momentum per nucleon between different MFs for both systems, with significantly higher net momenta for the MD than MI MFs, may be understood in terms of the violence of the explosion that accelerates the spectator.

An important aspect of the spectator momentum per nucleon, underscoring the interpretation above, is its dependence on the nucleon-nucleon cross section. In Fig. 9, the results of $b=6$ fm Au+Au simulation with the free cross sections are represented by filled symbols. With the larger free cross sections, the spectator remnants emerge even faster from the reaction than with the lower cross sections. This is because for higher cross sections, the equilibration is faster, which allows the participant to explode more violently when the spectators are still nearby. Quantitatively, in the $b=6$ fm HM free cross-section case, the gain in the longitudinal momentum per nucleon contributes as much as 17 out of 24 MeV/$c$ of the gain in the net spectator momentum per nucleon in Fig. 9. In the $b=6$ fm HM reduced cross-section case, the longitudinal gain contributes about 4 out of 8 MeV/$c$ of the net momentum gain per nucleon.

The mass and the excitation energy of the spectator in Figs. 4 and 5 do not exhibit a sensitivity to the EOS likely because they are determined by the geometry and the capability of matter to retain the energy, respectively. As to the momentum changes, though, we have demonstrated that they can provide information on the violent stage of energetic reactions and constrain the properties of high density nuclear matter.

## V. SUMMARY AND CONCLUSION

Within semiclassical transport simulations of energetic semicentral collisions of heavy ions, we have carried out an

investigation of the interplay between the participant and spectator regions. The spectators pass by the participant region when the participant matter undergoes a violent explosion. On one hand, the spectators block the expansion of the participant matter in the in-plane direction producing the elliptic flow for the participant matter. On the other hand, the explosion pushes the spectators giving them transverse momentum pointed away from the reaction zone. The momentum transfer to the spectators and the shadow left in the pattern of the participant emission depend on the speed of the explosion. The speed, in turn, depends on the EOS of the dense matter. Due to their nature, the spectators represent a perfectly timed probe right at the reaction site. A careful analysis of in-plane transverse momentum of a spectator may yield information on the EOS comparable to that provided by elliptic flow analysis. An analysis of the longitudinal momentum transfer may yield information on the momentum dependence of the MFs in the reactions. The signatures in the spectator momenta per nucleon rise with the lowering of the impact parameter, but at the cost of the lowering of a spectator mass, reducing the chances of identifying the spectator remnants. Significantly, for most repulsive MFs and low impact parameters in a heavy system, spectators may emerge from the reaction with a higher net average momentum per nucleon than the original momentum.

## ACKNOWLEDGMENTS

The authors would like to thank K.-H. Schmidt and B. Tsang for discussions. This work was partially supported by the National Science Foundation under Grant PHY-0070818 and by the Department of Energy under Grant DE-FGO2-87ER40331.A008.

[1] R. B. Wiringa, V. Fiks, and A. Fabrocini, Phys. Rev. C **38**, 1010 (1988).
[2] M. Liebendörfer, A. Mezzacappa, F.-K. Thielemann, O. E. B. Messer, W. R. Hix, and S. W. Bruenn, astro-ph/0006418.
[3] M. Prakash, I. Bombaci, P. J. Ellis, J. M. Lattimer, and R. Knorren, Phys. Rep. **280**, 1 (1997).
[4] D. Boyanovsky, hep-ph/0102120.
[5] G. F. Bertsch and S. Das Gupta, Phys. Rep. **160**, 189 (1988).
[6] T. Gaitanos, H. H. Wolter, and C. Fuchs, Phys. Lett. B **478**, 79 (2000).
[7] K. G. R. Doss, H. Å. Gustafsson, H. H. Gutbrod, K. H. Kampert, B. Kolb, H. Löhner, B. Ludewig, A. M. Poskanzer, H. G. Ritter, H. R. Schmidt, and H. Wieman, Phys. Rev. Lett. **57**, 302 (1986).
[8] H. Å. Gustafsson, H. H. Gutbrod, J. Harris, B. V. Jacak, K. H. Kampert, B. Kolb, A. M. Poskanzer, H. G. Ritter, and H. R. Schmidt, Mod. Phys. Lett. A **14**, 1323 (1988).
[9] H. H. Gutbrod, K. H. Hampert, B. Kolb, A. M. Poskanzer, H. G. Ritter, R. Schicker, and H. R. Schmidt, Phys. Rev. C **42**, 640 (1990).
[10] W. Reisdorf and H. G. Ritter, Annu. Rev. Nucl. Part. Sci. **47**, 663 (1997).
[11] R. Pak, D. Craig, E. E. Gualtieri, S. A. Hannuschke, R. A. Lacey, J. Lauret, W. J. Llope, N. T. B. Stone, A. M. Vander Molen, G. D. Westfall, and J. Lee, Phys. Rev. C **54**, 1681 (1996).
[12] P. Danielewicz and Q. Pan, Phys. Rev. C **46**, 2002 (1992).
[13] P. Danielewicz, Phys. Rev. C **51**, 716 (1995).
[14] P. Danielewicz, R. Lacey, P.-B. Gossiaux, C. Pinkenburg, P. Chung, J. M. Alexander, and R. L. McGrath, Phys. Rev. Lett. **81**, 2438 (1998).
[15] P. Danielewicz, Nucl. Phys. **A673**, 375 (2000).
[16] A. B. Larionov, W. Cassing, C. Greiner, and U. Mosel, nucl-th/0006009.
[17] J. Pochodzalla and W. Trautmann, nucl-ex/0009016.
[18] V. G. Bogdanov, V. A. Plyushchev, and Z. I. Solov'eva, Sov. J. Nucl. Phys. **53**, 557 (1991).
[19] G. M. Chernov *et al.*, Nucl. Phys. **A412**, 534 (1984).
[20] D. J. Morrisey, Phys. Rev. C **39**, 460 (1989).
[21] J. D. Bowman, W. J. Swiatecki, and C.-F. Tsang, Lawrence Berkeley Laboratory Report No. LBL-2908, 1973 (unpublished).
[22] G. Westfall *et al.*, Phys. Rev. Lett. **18**, 1202 (1976).
[23] J. Gosset, H. H. Gotbrod, W. G. Meyer, A. M. Poskanzer, A. Sandoval, R. Stock, and G. D. Westfall, Phys. Rev. C **16**, 629 (1977).
[24] A. Schüttauf *et al.*, Nucl. Phys. **A607**, 457 (1996).